A Numerical Model for the Transport of Reactants in Proton Exchange Fuel Cells

Abel Rubio
Faculty of Electrical and Computer Engineering, CASE, CIDIS
Escuela Superior Politécnica del Litoral, ESPOL
Guayaquil, Ecuador
grubio@espol.edu.ec
ORCID: 0000-0002-6057-4909

Wilton Agila
Faculty of Engineering in Electricity and Computation, CASE, CIDIS Escuela Superior Politécnica del Litoral, ESPOL
Guayaquil, Ecuador
wagila@espol.edu.ec
ORCID: 0000-0002-8117-7777

Leandro González
The Centre for Automation and Robotics
Madrid, España
leandro.gonzalez@car.upm-csic.es

Jonathan Aviles
Faculty of Engineering in Electricity and Computation, FIEC
Escuela Superior Politécnica del Litoral, ESPOL
Guayaquil, Ecuador
joabavil@espol.edu.ec
ORCID: 0000-0002-3386-0643

2023 12th International Conference on Renewable Energy Research and Applications (ICRERA) | 979-8-3503-3793-8/23/$31.00 ©2023 IEEE | DOI: 10.1109/ICRERA59003.2023.10269354

***Abstract*— Energy has allowed the development of our society and currently, the hydrogen-powered fuel cell is the most promising energy source of the future since it would help to eliminate serious problems such as climate change and economic inequality. The fuel cell converts the chemical energy of the reactants used into electrical energy and produces water and heat as by-products during its operation. The proton exchange membrane fuel cell is expected to play a key role in the future energy system due to its favourable characteristics and its application in mobile phones, electric vehicles, distributed power systems, submarines and aerospace applications. To optimize the operation of the fuel cell, models have been developed that represent it as a structural, dimensional, thermal and state system, which requires —as a contribution to technological development—, a strategic and systemic vision. The document analyzes the technique of numerical methods, to ensure optimal operation of the Proton exchange membrane fuel cell, addressing non-linearities of electrical behaviour and the imprecision of the physical world.**

Keywords—Sustainability, renewable energy, economic inequality

Abbreviations

2D	Two dimensions
3D	Three dimensions
CFD	Computer fluid dynamic
GDL	Gas diffusion layer
LBM	Lattice Boltzmann method
NS	Navier-Stokes
PEMFC	Proton exchange membrane fuel cell
PEM	Proton exchange membrane
PNP	Poisson–Nernst–Planck
PSPC	Partially separated-partially coupled
PTFE	Polytetrafluoroethylene
VOF	Volume of fluid

I. Introduction

The fuel cell is one of the pillars to achieve an economy based on renewable energies [1,2] and its optimization has been a great challenge that, to achieve it, has used stochastic methods [3], approximate reasoning techniques [4, 5], fuzzy logic [6], distributed intelligence for autonomous control of the stack [7] and artificial intelligence with different algorithms. Mathematical modelling techniques allow analysing variables and parameters related to temperature, pressure, reagent moisture, membrane moisture, and electrochemical reactions [8].

The non-uniform distribution of flows in PEMFC cells occurs when several cells are assembled to obtain high output powers. This problem causes flooding and hot spots that end up affecting battery life and performance. To study the distribution of flows and droplet dynamics, it is preferred to use mathematical modelling and numerical simulations, including Volume of Fluid (VOF), Lattice Boltzmann (LBM) and optical photography, to reduce costs and complexities on a small scale [9]. Numerical methods have allowed us to analyze different types of channels, condensation and water transport in the perforated and non-perforated GDL diffusion layers, and even their deformation due to the pressure exerted in the assembly process [10].

One of the works of flow field analysis in the collecting channel used the analytical model of multiple flow volumetric balance instead of the macroscopic energy balance and proposed an analytical model with a simple and numerically validated criterion, which allowed to determine the uniformity of flows [11]. On the other hand, a two-block channel for mass transport in the cathode channel showed that, under different operating conditions, the stack improves its performance [12]. Another study developed a new channel for the cathode, partially separated-partially coupled (PSPC), considering that a good flow field at the cathode reduces heat and mass transfer losses. The results indicated improvements in the removal of water from the cathode and improvements in the distribution of heat and water, obtaining a 13.5% higher current density than would be obtained with independent cooling channels [13].

In the same line of the analysis of the flow fields, the condensation mode and condensation circulation mode were applied to reduce the amount of liquid-water in the anode and reduce the risk of flooding of the PEMFC. The results of the condensation circulation mode are better than those of the circulation mode [14]. The PEMFC with a dead-end anode allows efficient use of hydrogen, besides that the hydrogen supply systems are simple [15].

Regarding the flows in the GDL, these depend on the design of the channels and the construction of the GDL. The GDL can be of a single layer —macroporous— or of a double layer —macroporous and microporous—. The macroporous layer serves to distribute the gases and collects the current and the microporous to manage the flow of water [16]. One of the investigations analyzed the gas-liquid flow with a VOF-3D model and different charges of polytetrafluoroethylene (PTFE) —widely used to improve the hydrophobicity of GDLs—. The predictions were compared with the LBM and with the experimental results and allowed to contribute to the study of the effects of PTFE on water dynamics [17]. Another of the studies analyzed the heat and mass transfer in the GDL using a gas-liquid-solid model. The results indicated that liquid water transport has a low impact on electrical conduction and that the model can provide a temperature distribution in a compressed DOF [18].

The objective of this work is to develop a mathematical model that, solved numerically using Octave —computing language oriented to matrix numerical calculation—, allows us to graphically understand the behaviour of electrical potential; of the conductivity, density and distribution of electrical density at the electrode-membrane border. The model does not consider the effect of the membrane and assumes that the charge accumulates on the electrode surface, originating in the Gouy-Chapman-Stern double layer.

II. THE MATHEMATICAL MODEL FOR PEMFC

The transport of the reactants hydrogen and oxygen is carried out through the gas flow channels and the gas diffusing layers[19].

A. Transport through gas flow channels

The gas diffusion channels are normally made of non-porous graphite and have characteristics such as adequate channelling to allow the passage of reactants from the ducts to the electrodes and to evacuate the water from the cell. They are chemically stable because they are in contact with hydrogen and oxygen and have high electrical conductivity, mechanical resistance, and thermal conductivity.

Since the gas transport is related to the geometry of the channels, which is in the scale of mm or cm, for the analysis of mass transport, concepts related to the convection process are required; that is, fluid dynamics [20]. Consequently, it is an application of the conservation theorem to the fluid flow process and this in turn allows defining of the motion of a particle in a fluid through the Navier-Stokes equations [21,22]:

$$\frac{\partial \boldsymbol{v}}{\partial t} + (\boldsymbol{v} \cdot \boldsymbol{\nabla})\boldsymbol{v} = -\frac{1}{\rho_f}\boldsymbol{\nabla}_p + \upsilon \nabla^2 \boldsymbol{v} \quad (1)$$

Where:

η: Dynamic viscosity
ξ: Volumetric viscosity
υ: Kinematic viscosity
ρ_f: Fluid density
$\boldsymbol{v}$: Fluid velocity.

B. Transport of reactants through the gas-diffusing layers

The diffusion layers evenly distribute the reactants to the catalyst layer and provide good electrical contact, both with the catalyst layers across the entire surface and with the gas diffusion channels. They are usually made of carbon paper with Teflon, coated with a platinum-containing catalyst to improve the speed and efficiency of the electrochemical reaction that occurs there and consequently obtain a high current [23].

Since the gas transport is related to the structures and porosities of the diffusing layers which are in the [µm] or [nm] scale, it mainly requires concepts related to the diffusion process. The motion of a particle in diffusion is defined by the Nernst-Planck equations, therefore:

$$\frac{\partial C_i}{\partial t} + \boldsymbol{v_f}.\boldsymbol{\nabla} C_i - D\nabla^2 C_i = \frac{\partial C_i}{\partial t} + \left(C_i \boldsymbol{\nabla}.\boldsymbol{v_f} + \boldsymbol{v_f}.\boldsymbol{\nabla} C_i\right) - D\nabla^2 C_i = \mathbf{0} \quad (2)$$

If the flow is incomprehensible $\boldsymbol{\nabla}.\boldsymbol{v_f} = \mathbf{0}$ (and having considered diffusion-convection):

$$\frac{\partial C_i}{\partial t} + \boldsymbol{v_f}.\boldsymbol{\nabla} C_i = D\nabla^2 C_i \quad (3)$$

Due to the complexity and limitations to measuring transport phenomena within porous media -particularly in PEMFCs-, numerical simulations with CFD, the Boltzmann grid method [24], the Fick and Maxwell diffusion equations–Stefan [25] and the pore network have received such attention that the microstructure of porous materials can now be accurately reconstructed [26].

C. Numerical model

To better appreciate the physical-chemical behaviour of the PEM fuel cell and facilitate the solution of the transport problem, the equations are written in a dimensionless form, being able to describe the phenomena regardless of the magnitude of the scales. The Navier-Stokes and Poisson-Nernst-Planck (NS-PNP) equations that model the fuel cell are:

$$\frac{\partial \boldsymbol{v}}{\partial t} + \boldsymbol{v} \cdot \nabla \boldsymbol{v} = -\boldsymbol{\nabla_p} + \frac{1}{R_e}\boldsymbol{\nabla}^2 \boldsymbol{v} \quad (4)$$

$$\boldsymbol{\nabla}.\boldsymbol{v} = 0 \quad (5)$$

$$-\epsilon^2 \boldsymbol{\nabla}^2 \varphi = \rho_q \quad (6)$$

$$\frac{\rho_q}{\partial t} + \boldsymbol{v_{conv}} \cdot \boldsymbol{\nabla}\rho_q = \frac{1}{P_e}\boldsymbol{\nabla}.\left(\boldsymbol{\nabla}\rho_q + \sigma\boldsymbol{\nabla}\varphi\right) \quad (7)$$

$$\frac{\sigma}{\partial t} + \boldsymbol{v_{conv}} \cdot \boldsymbol{\nabla}\sigma = \frac{1}{P_e}\boldsymbol{\nabla}.(\boldsymbol{\nabla}\sigma + \rho_q\boldsymbol{\nabla}\varphi) \quad (8)$$

Where:

$$R_e = \frac{\rho_f \boldsymbol{v} D_h}{\eta} \quad (9)$$

$$R_{el} = \frac{\rho v_{ref}^2}{RTC_{ref}} \quad (10)$$

$$P_e = \frac{hv_{ref}}{D} \quad (11)$$

$$\epsilon = \frac{\lambda_D}{h} \quad (12)$$

$$\lambda_D = \sqrt{\frac{\epsilon_S RT}{z^2F^2C_{ref}}} \quad (13)$$

R_e is the Reynolds number for rectangular channels, R_{el} is the electric Reynolds number, P_e Péclet number and λ_D Debye length.

The boundary conditions (electrodes) are:

$$\boldsymbol{v} = 0 \quad (14)$$

$$\frac{\boldsymbol{\lambda s}}{\boldsymbol{h}}\boldsymbol{\nabla\varphi}\,.\,\boldsymbol{n} = \boldsymbol{V_z} \quad (\mathbf{15})$$

$$\left(\boldsymbol{\nabla\rho_q} + \boldsymbol{\sigma\nabla\varphi}\right).\,\boldsymbol{n} = -\boldsymbol{R}\left(\boldsymbol{\sigma},\boldsymbol{\rho_q},\boldsymbol{V_z}\right) \quad (\mathbf{16})$$

$$\left(\boldsymbol{\nabla\sigma} + \boldsymbol{\rho_q\nabla\varphi}\right).\,\boldsymbol{n} = -\boldsymbol{R}\left(\boldsymbol{\sigma},\boldsymbol{\rho_q},\boldsymbol{V_z}\right) \quad (\mathbf{17})$$

If the flow develops completely at the entrance or exit of the channel, the boundary conditions would be:

$$\boldsymbol{pn} - \frac{\mathbf{1}}{\boldsymbol{R_e}}\boldsymbol{\nabla v}\,.\,\boldsymbol{n} = \mathbf{0} \quad (\mathbf{18})$$

$$\boldsymbol{\nabla\varphi}\,.\boldsymbol{n} = \boldsymbol{\nabla\sigma}\,.\boldsymbol{n} = \boldsymbol{\nabla\rho_q}\,.\boldsymbol{n} = \mathbf{0} \quad (\mathbf{19})$$

D. Case 1: Stable NS-PNP solution (v=0)

Assuming that λ_S is a "macroscopic distance" the charge density is small compared to the total concentration and therefore, $\rho_q \cong 0$ *and* $\epsilon = \frac{\lambda_D}{h} \to 0$. From the NS equations, if $v = 0$:

$$\mathbf{0} = -\boldsymbol{\nabla_p} \quad (\mathbf{20})$$

While those of PNP are reduced to:

$$\boldsymbol{\epsilon^2\nabla^2\varphi} = \mathbf{0} \quad (\mathbf{21})$$

$$\boldsymbol{\nabla}\,.\,(\boldsymbol{\sigma\nabla\varphi}) = \mathbf{0} \quad (\mathbf{22})$$

$$\boldsymbol{\nabla^2\sigma} = \mathbf{0} \quad (\mathbf{23})$$

In the interval: $-1 + \delta \le y \le 1 - \delta$

In the asymptotic regime, $\delta \approx 0$ and assuming that there are only variations in the direction, the slope is proportional to the current direction j. Finally:

$$\boldsymbol{\sigma} = \mathbf{0.5} - \boldsymbol{jx} \quad (\mathbf{24})$$

In terms of In terms of σ_-:

$$\boldsymbol{\sigma} = \boldsymbol{\sigma_-} + \boldsymbol{j}(\mathbf{1} - \boldsymbol{x}) \quad (\mathbf{25})$$

Similarly:

$$\boldsymbol{\varphi}(\boldsymbol{x}) = \boldsymbol{\varphi_-} + \boldsymbol{ln}\left(\frac{\boldsymbol{\sigma}}{\boldsymbol{\sigma_-}}\right) \quad (\mathbf{26})$$

The current limit j=0.5 corresponds to zero conductivity at the cathode and φ satisfies Poisson's equation (7) only if:

$$\boldsymbol{\rho_q} = \boldsymbol{j}\left(\frac{\boldsymbol{\epsilon}}{\boldsymbol{\sigma}}\right)^{\mathbf{2}} \quad (\mathbf{27})$$

E. Case 2: Dynamic NS-PNP solution (v=0)

For this case (which is a generalization of case 1), the solution of NS is decoupled from the PNP equations. If v satisfies the NS equations, the stationary solution for σ and φ satisfies the PNP equations. When $\rho_q = 0$ the PNP equations reduce to:

$$-\epsilon^2\boldsymbol{\nabla}^2\varphi = 0 \quad (28)$$

$$\boldsymbol{\nabla}\,.\,(\boldsymbol{\sigma\nabla\varphi}) = \mathbf{0} \quad (29)$$

$$\boldsymbol{v_{conv}}\,.\boldsymbol{\nabla}\sigma - \frac{1}{P_e}\nabla^2\sigma = 0 \quad (30)$$

Case 2.1: v=(0,1):

This case leads to the equations:

$$\boldsymbol{\nabla}\,.\,(\sigma\boldsymbol{\nabla}\varphi) = 0 \quad (31)$$

$$\nabla\sigma - \frac{1}{P_e}\nabla^2\sigma = 0 \quad (32)$$

$$\frac{\partial\sigma}{\partial y} = \frac{1}{P_e}\left(\frac{\partial^2\sigma}{\partial x^2} + \frac{\partial^2\sigma}{\partial y^2}\right) \quad (33)$$

With boundary conditions:

$$\boldsymbol{\sigma}(-\mathbf{1},\boldsymbol{y}) = \boldsymbol{\sigma_+} \quad (\mathbf{34})$$

$$\boldsymbol{\sigma}(\mathbf{1},\boldsymbol{y}) = \boldsymbol{\sigma_-} \quad (\mathbf{35})$$

$$\boldsymbol{\sigma}(\boldsymbol{x},\mathbf{0}) = \begin{cases}\boldsymbol{\sigma_+}\ \boldsymbol{si} - \mathbf{1} \le \boldsymbol{x} < \mathbf{0},\\ \boldsymbol{\sigma_-}\ \boldsymbol{si} - \mathbf{0} \le \boldsymbol{x} < \mathbf{1}\end{cases} \quad (\mathbf{36})$$

If the cell is long then Pe is small and the solution is that of case 1. Assuming that σ(x,y) has a natural and a forced component:

$$\boldsymbol{\sigma}(\boldsymbol{x},\boldsymbol{y}) = \boldsymbol{\sigma_n}\,(\boldsymbol{x},\boldsymbol{y}) + \boldsymbol{\sigma_f}(\boldsymbol{x}) \quad (\mathbf{37})$$

Where $\sigma_f(x)$ is the stable solution ($v = 0$)

$$\boldsymbol{\sigma_f}(\boldsymbol{y}) = \boldsymbol{\sigma_-} + \boldsymbol{j}(\mathbf{1} - \boldsymbol{x})\ ;\ \mathbf{0} < \boldsymbol{j} \le \mathbf{0.5} \quad (\mathbf{38})$$

$\sigma_n\,(x,y)$ is the transient solution that decays exponentially in x, that is, $\lim_{x\to\infty}\sigma_n(x,y) = 0$. The method of separation of

variables can be applied to convert the partial differential equation into ordinary differential equations and the solution is expressed in the form:

$$\boldsymbol{\sigma_n(x,y)} = \sum_{n=1}^{\infty} \boldsymbol{C_n}\, \boldsymbol{e}^{\left(-\frac{P_e}{2}\right)\left[\sqrt{1+\left(\frac{(2n-1)\pi}{P_e}\right)^2}-1\right]y}\, \boldsymbol{sen}((\boldsymbol{2n-1})\,\boldsymbol{\pi})\boldsymbol{x} \quad (39)$$

$$\boldsymbol{C_n} = \boldsymbol{j}\left[\frac{\boldsymbol{2}}{\boldsymbol{n}}(\boldsymbol{-1})^{\boldsymbol{n+1}}\right] + \frac{\boldsymbol{2}}{\boldsymbol{2n-1}}\,(\,\boldsymbol{\sigma_-} - \boldsymbol{\sigma_+}) \qquad (40)$$

III. ANALYSIS OF RESULTS

Graphs 1, 2 and 3 do not present labels on their axes, because their equations were written in a dimensionless form, precisely to describe the phenomena regardless of the magnitude of the scales.

The graph. 1 describes the results for case 1, that is, the curves of the electrical conductivity σ, of the charge density ρ_q and of the electrical potential φ. Analysing the graph of the potential for various values of *Jv*, it is observed that $j = 0.5$ represents zero conductivity at the cathode.

Graphs 2 and 3 present the result for the dynamic NS-PNP solution (v = 0). From the graphs, an overshoot and an undershoot in the electrical conductivity can be observed. The model describes the dynamic operation of the PEMFC considering the transients produced by the transport of the reactants and by the electrochemical reactions.

The results are validated with those obtained by other analyses, in which the equation had a different form; for example, with the results obtained by [27] who found the following equations:

$$\sigma(x,y) = \sigma_- + j(y+1) + (\sigma_+ - \sigma_-)\sum_{n=1}^{\infty} C_n\, e^{-\frac{P_e}{2}\left(\sqrt{1+\left(\frac{n\pi}{P_e}\right)}-1\right)x}\, sin\left(\frac{n\pi}{2}(y+1)\right) \quad (41)$$

$$C_n = \frac{2}{n\pi}(\sigma_+ - \sigma_-)\, cos\left(\frac{n\pi}{2}\right) \qquad (42)$$

Where it is observed that the exponential factor is the same, but not the sinusoidal function or the value of the power series.

IV. CONCLUSIONS

If the numerical models are considered, they have allowed validation of the dynamic response of the electrical conductivity of the fuel cell, both for the stationary state and for the dynamic state considering a 2D model, in the (x,y) plane, obtaining the respective surface curve in which an overshoot and an undershoot of electrical conductivity can be observed. These transients must be considered if adequate and efficient control of the PEMFC is required.

REFERENCES

[1] A. Rubio, W. Agila, L. González, M. Ramirez and H. Pineda, "A Critical Analysis of the Impact of the Pandemic on Sustainable Energy Scenarios," 2023 11th International Conference on Smart Grid (icSmartGrid), Paris, France, 2023, pp. 01-07, doi: 10.1109/icSmartGrid58556.2023.10171066.

[2] A. Rubio, W. Agila, "Sustainable Energy: A Strategic Overview of Fuel Cells", IEEE, International Conference on Renewable Energy Research and Applications (ICRERA), Brasov Rumania, November 2019, pp. 1044-1048.

[3] Jiao, D., Jiao, K., & Du, Q. (2021). Numerical investigations of vapour condensation and water transport in gas diffusion layers of PEMFC. International Journal of Heat and Mass Transfer, 177, 121543. doi.org/10.1016/j.ijheatmasstransfer.2021.121543

[4] W. Agila, G. Rubio, J. Aviles-Cedeno and L. González, "Approximate Reasoning Techniques in the Control of States of Operation of the PEM Fuel Cell," 2023 11th International Conference on Smart Grid (icSmartGrid), Paris, France, 2023, pp. 1-6, doi: 10.1109/icSmartGrid58556.2023.10170778.

[5] W. Agila, G. Rubio, L. Miranda, L. Vázquez, "Qualitative Model of Control in the Pressure Stabilization of PEM Fuel Cell", 2018 7th International Conference on Renewable Energy Research and Applications (ICRERA), Paris France, October 2018, pp. 1221-1226.

[6] G.A. Rubio, W.E. Agila, "A Fuzzy Model to Manage Water in Polymer Electrolyte Membrane Fuel Cells", Processes 2021, 9, 904. https://doi.org/10.3390/pr9060904

[7] A. Rubio, W. Agila, L. González, J. Aviles-Cedeno, "Distributed Intelligence in Autonomous PEM Fuel Cell Control", Energies 2023, 16, 4830. https://doi.org/10.3390/en16124830.

[8] Omran, A., Lucchesi, A., Smith, D., Alaswad, A., Amiri, A., Wilberforce, T., ... & Olabi, A. G. (2021). Mathematical model of a proton-exchange membrane (PEM) fuel cell. International Journal of Thermofluids, 11, 100110.

[9] Xu, S., Liao, P., Yang, D., Li, Z., Li, B., Ming, P., & Zhou, X. (2023). Liquid water transport in gas flow channels of PEMFCs: A review on numerical simulations and visualization experiments. International Journal of Hydrogen Energy, 48(27), 10118-10143. doi.org/10.1016/j.ijhydene.2022.12.140

[10] Jiao, D., Jiao, K., Du, Q., "Numerical investigations of vapor condensation and water transport in gas diffusion layers of PEMFC", International Journal of Heat and Mass Transfer, 177, 2021, 121543. doi.org/10.1016/j.ijheatmasstransfer.2021.121543

[11] Pan, W., Chen, Z., Chen, X., Wang, F., Dai, G., "Analytical and numerical investigation of flow distribution in PEMFC stacks", Chemical Engineering Journal, 450, 2022, 137598. https://doi.org/10.1016/j.cej.2022.137598

[12] Dong, Z., Qin, Y., Zheng, J., Guo, Q., "Numerical investigation of novel block flow channel on mass transport characteristics and performance of PEMFC", International Journal of Hydrogen Energy, 2023. doi.org/10.1016/j.ijhydene.2023.03.258

[13] Chen, C., Wang, C., & Zhang, Z. (2022). A novel channel design and heat and mass transfer analysis of fuel cells. Energy Conversion and Management, 254, 115273. doi.org/10.1016/j.enconman.2022.115273

[14] Huang, Z., Jian, Q., Zhao, J., "Experimental study on improving the dynamic characteristics of open-cathode PEMFC stack with dead-end anode by condensation and circulation of hydrogen", International Journal of Hydrogen Energy, 45(38), 2020, 19858-19868. doi.org/10.1016/j.ijhydene.2020.05.108

[15] Chen, B., Liu, Q., Zhang, C., Liu, Y., Shen, J., Tu, Z., "Numerical study on water transfer characteristics under joint effect of placement orientation and flow channel size for PEMFC with dead-ended anode", Energy, 254, 2022, 124365. doi.org/10.1016/j.energy.2022.124365

[16] Al-Okbi, Y., Al-murshedi, A., Nemah, M., Saad, H., "Influence of design anode and cathode channel on (PEMFC) fuel cell performance", Materials Today: Proceedings, 42, 2021, 2177-2184. doi.org/10.1016/j.matpr.2020.12.302

[17] Niu, Z., Wu, J., Bao, Z., Wang, Y., Yin, Y., Jiao, K., "Two-phase flow and oxygen transport in the perforated gas diffusion layer of proton exchange membrane fuel cell", International Journal of Heat and Mass Transfer, 139, 2019, 58-68. doi.org/10.1016/j.ijheatmasstransfer.2019.05.008

[18] D. Jiao, K. Jiao, S. Zhong, Q. Du, "Investigations on heat and mass transfer in gas diffusion layers of PEMFC with a gas–liquid-solid coupled model. Applied Energy, 316, 2022, 118996. https://doi.org/10.1016/j.apenergy.2022.118996

[19] A. Rubio, W. Agila, "Dynamic Model of Proton Exchange Membrane Fuel Cells: A Critical Review and a Novel Model", IEEE, International Conference on Renewable Energy Research and Applications (ICRERA), Brasov Rumania, November 2019, pp. 353-358.

[20] I. Khazaee, “Improvement the equation of polarization curve of a proton exchange membrane fuel cell at different channel geometry”, Heat and Mass Transfer, Vol. 51, No.12, 2015, pp. 1681-1689.

[21] J. Morales, C. Astorga, J. Reyes, U. Cano y P. Cruz, “Application of a nonlinear observer for estimation of variables in a PEM fuel cell system”, Journal of the Brazilian Society of Mechanical Sciences and Engineering, Vol. 39, No. 4, 2017, pp. 1323-1332.

[22] A. Rubio, W. Agila, “A Novel System-Level Model for a Fuel Cell in a Strategic Context”. In Proceedings of the 2018 7th International Conference on Renewable Energy Research and Applications (ICRERA), Paris, France, 14–17 October 2018, pp. 1044–1048.

[23] M. Pérez, “Estudio del comportamiento estacionario y dinámico de una pila de combustible tipo pem de 300 w operando en los modos ánodo cerrado o dead-end y ánodo abierto”, tesis doctoral, Universidad Politécnica de Valencia, 2012.

[24] A. Xu, W. Shyy y T. Zhao, "Lattice Boltzmann modeling of transport phenomena in fuel cells and flow batteries", Acta Mechanica Sinica, 2017, pp. 1-20.

[25] M. Lindstrom y B. Wetton, "A comparison of Fick and Maxwell–Stefan diffusion formulations in PEMFC gas diffusion layers", Heat and Mass Transfer, Vol. 53, No. 1, 2017, pp. 205-212.

[26] Y. Kawagoe, T. Oshima, K. Tomarikawa, T. Tokumasu, T. Koido y S. Yonemura, "A study on pressure-driven gas transport in porous media: from nanoscale to microscale", Microfluidics and Nanofluidics, Vol. 20, No. 12, pp. 162, 2016.

[27] M. González, “Estudio de las ecuaciones de Poisson-Nernst-Planck y algunas de sus aplicaciones”, tesis de maestría en matemáticas aplicadas, Universidad Autónoma Metropolitana, México, 2011.

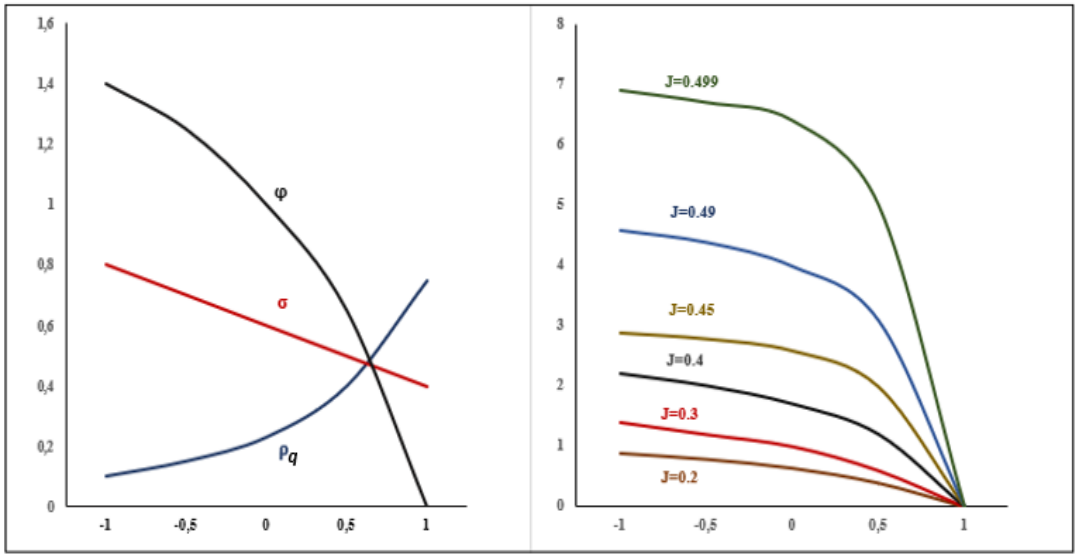

Fig. 1 Potential, conductivity, charge density, and electric potential

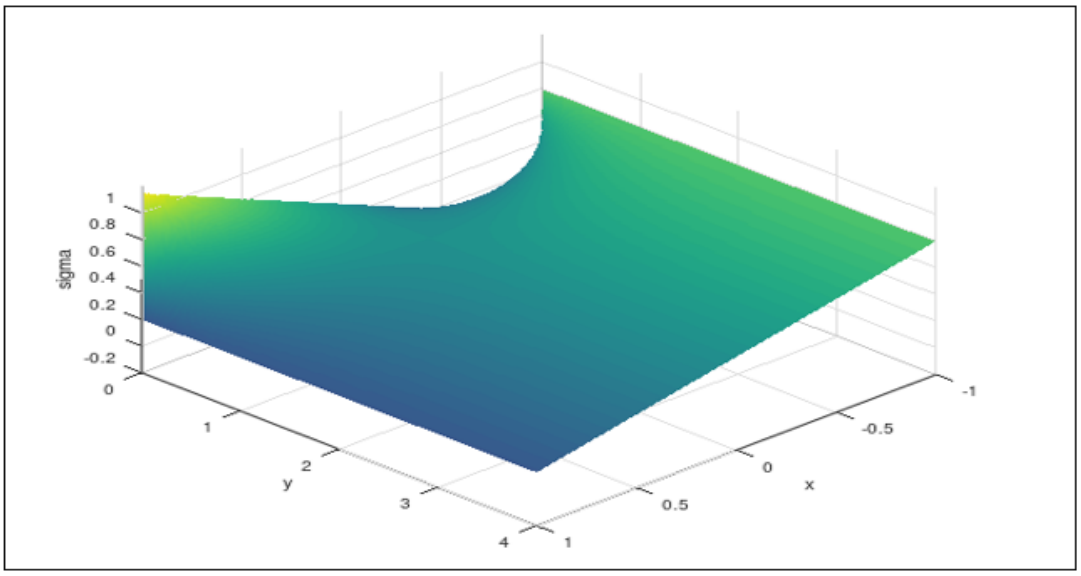

Fig. 2 Dynamic NS-PNP solution (v = 0)

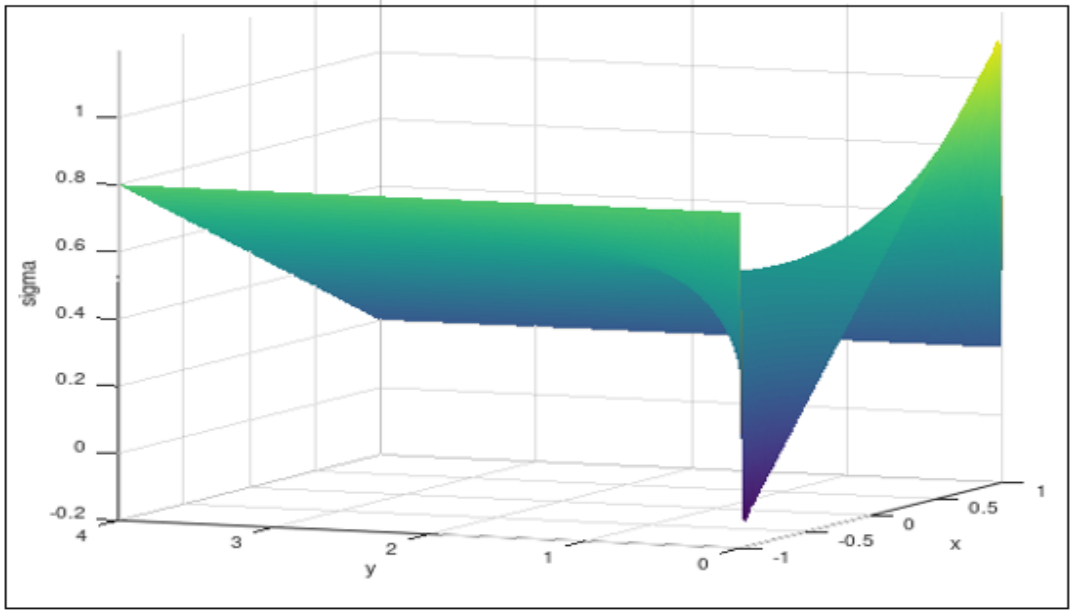

Fig.3 Dynamic NS-PNP solution (v = 0)